

Nonlinear Dynamics of Coupled Nickel Electrodissolution with Hydrogen Ion Reduction with Bipolar Electrodes

To cite this article: Yifan Liu and István Z. Kiss 2023 J. Electrochem. Soc. 170 113505

View the article online for updates and enhancements.

You may also like

 Investigation of IrO₂ Stability As a Cell-Reversal Mitigation Catalyst in PEMFC Anodes

Ana Marija Damjanovia, Mohammad Fathi Tovini, Anna Freiberg et al.

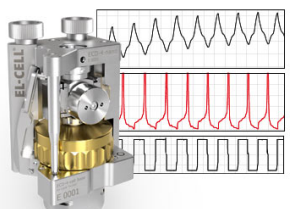
- A Novel Way to Determine the Product Distribution from Parasitic Methanol Oxidation Reaction on Oxygen Reduction Reaction Catalysts

Reaction Catalysts
Tilman Jurzinsky, Philipp Kurzhals,
Karsten Pinkwart et al.

- A Simple, One-Dimensional Electrochemical Model for the Lithium-Sulfur Battery

Sevgi Can Erensoy and Damla Eroglu

Measure the Electrode Expansion in the Nanometer Range. Discover the new ECD-4-nano!



- Battery Test Cell for Dilatometric Analysis (Expansion of Electrodes)
- Capacitive Displacement Sensor (Range 250 µm, Resolution ≤ 5 nm)
- Detect Thickness Changes of the Individual Electrode or the Full Cell.

www.el-cell.com +49 40 79012-734 sales@el-cell.com









Nonlinear Dynamics of Coupled Nickel Electrodissolution with Hydrogen Ion Reduction with Bipolar Electrodes

Yifan Liu and István Z. Kiss^z

Department of Chemistry, Saint Louis University, St. Louis, Missouri 63103, United States of America

We investigate the emergence of current oscillations of a bipolar electrode (BPE) in coupled anode/cathode reaction under potentiostatic condition. In a traditional three-electrode setup, the nickel dissolution in sulfuric acid requires a minimum amount of IR ohmic drop, and thus series resistance for the oscillations to occur. In this paper, it is shown that in bipolar setup, when the nickel electrodissolution on the anodic side is coupled to hydrogen ion reduction on the cathodic side, spontaneous current oscillations can occur. An electrochemical analysis of the dynamics shows that the required circuit potential for the oscillations can be predicted from estimating the overpotentials needed for the anodic and cathodic reactions, the driving electrode, and the ohmic drop in the electrolyte. The dynamics and range of oscillations can be tuned by different concentrations of electrolyte, on both the anodic and the cathodic sides. In the considered example, the charge transfer resistance of the cathodic reaction can provide sufficient total resistance even when the solution resistance does not yield sufficient IR drop for the oscillations. Our findings have the potential to promote further studies of the collective behavior of electrochemical reactions using multielectrode arrays in bipolar electrode setups.

© 2023 The Electrochemical Society ("ECS"). Published on behalf of ECS by IOP Publishing Limited. [DOI: 10.1149/1945-7111/ad0baf]

Manuscript submitted August 18, 2023; revised manuscript received October 29, 2023. Published November 23, 2023.

Electrochemical systems exhibit a variety of nonlinear phenomena, which are often investigated in traditional cells.¹ conventional electrochemical cell involves three (working, counter, and reference) or two (working and the same counter/reference) electrodes, where a circuit potential is applied between the working and counter electrode such that the potential between the working and reference electrode is constant.³ In the commonly used threeelectrode setup, the given electrode reaction on the working electrodes can be studied with little influence from the counter electrode. (Similarly, with large surface area counter electrode, the potential drop on the counter electrode can be neglected even without a reference electrode/potentiostat, and thus the electrode kinetics of the working electrode is decoupled from that the of counter electrode.) In such configuration, various forms of stationary and oscillatory patterns have been observed on the surface of a single electrode 4-6 and multielectrode arrays. 7-9 Shrinking down the size of the reactor from macro- to microscale enables the discovery of new dynamic features¹⁰, and further decreasing the size to nanoscale helps for better understanding of the mechanisms of electrochemical reactions.^{11–13} However, problems also arise at nanoscale, for example, making direct electrical contact to nanoelectrodes is often difficult.

Bipolar electrochemistry is an unconventional technique that involves two driving electrodes and a conducting object (the bipolar electrode, BPE) in electrolytic solution. 14-16 Compared to conventional electrochemical cell, bipolar electrodes are distinctly different in that they promote oxidation and reduction simultaneously on the same electrode which acts both as anode and cathode.¹⁷ The anode of the bipolar electrode is the cathode side of the driving electrode, and vice versa. 18 A bipolar electrode does not need direct contact with an external wire to a power source, which makes it ideal for nanoelectrochemistry. Studies on single bipolar nanoelectrode¹⁹ and on array of hundreds of ultramicroelectrodes²⁰ are thus enabled. When the driving potential is large enough (larger than the formal potential of the anodic and cathodic reactions), both oxidation and reduction occur at the two ends of the electrode, making the electrode bipolar. Thus, the anodic and cathodic reactions are naturally coupled through the BPE. The theoretical and experimental current-potential responses of a micro BPE under mass-transport control have been characterized in different concentrations of electrolyte.²¹ For applications of BPE in practical settings, the analysis of the nonlinear dynamics of coupled cathode-anode systems can reveal the type of self-organized spatio-temporal

structures that can affect the dominant dynamical response of the cell

Coupled anode-cathode reactions have been utilized as a promising green method for organic synthesis.²² It is possible to produce desirable products simultaneously at both anode and cathode sides, which optimizes the energy efficiency. 23,24 The nonlinear dynamics of a coupled anode-cathode system, nickel electrodissultion and hydrogen ion reduction, was explored in a previous study²⁵ in a traditional two electrode system. Bistability and current oscillations were observed due to the interaction of the reactions. The results were interpreted by the kinetics of the relatively slow anodic metal dissolution coupled to the fast cathodic reaction. As a result of the complex kinetics of the cathode reaction, the charge transfer resistance exhibited a maximum value by changing the cathode sizes; the instabilities were then interpreted with this increased additional ohmic drop needed to drive the cathodic reaction. In another work, 26 coupled dual-anode and single-cathode configuration was used to characterize the synchronization pattern for an oscillatory reaction. The coupling effect was demonstrated with in-phase, out-of-phase, and anti-phase synchronization in smooth, relaxation, or chaotic current oscillations. The coupling pattern was found to be induced by the cathode and was interpreted with the ratio of charge transfer resistance of the cathode to the total external resistance in the cell. A further study² demonstrated quorum sensing transitions to current oscillations in a coupled multi-anode and single-cathode system. The number of anode electrodes in the system played similar role to population density in quorum sensing: with increasing or decreasing the population density a transition to current oscillation occurred. The type of the transition depended on the extent of nonlinearity of the oscillations: while relaxation oscillation exhibited regular quorum sensing (oscillations occurred with increasing population density), smooth oscillators demonstrated "inverse" quorum sensing (oscillations via decreased population density). In these results. 25-27 both cathode and anode reside in the same container and share common electrolyte.

In this paper, a closed bipolar electrode is used to investigate the nonlinear dynamics of coupled cathode-anode reactions. A closed BPE is built with a U-cell where two compartments are separated by the BPE in the middle. The nickel electrodissolution in sulfuric acid, coupled to hydrogen ion reduction, is studied with different electrolyte concentrations at the anode and cathode sides. Polarization scans are performed to determine the circuit potential range and current levels of the oscillations. Electrochemical impedance spectroscopy is used to determine the charge transfer resistance of cathodic reaction and the solution resistance. The

results are interpreted by the interplay of the negative differential resistance of the anode and the total resistance composed of charge transfer and solution resistances. With the assumption that the oscillations are induced by the total cell resistance, the results are compared to those obtained in traditional three-electrode configurations with applications of external resistance. The success of the approach to decode oscillatory instabilities is demonstrated in three different electrolyte configurations with changes in both the anodic and cathodic sides. The advantages of using BPE for exploring dynamical instabilities of coupled anode and cathode reactions are discussed.

Materials and Methods

Two different configurations were used: one is the traditional three-electrode cell, and the other is the bipolar electrode in U-cell. The experimental setup of a three-electrode traditional cell is shown in Fig. 1a. The electrochemical cell consisted of the electrolyte (H₂SO₄), a counter electrode (CE, platinum coated titanium rod), a reference electrode (RE, Hg/Hg₂SO₄ sat. K₂SO₄), and a working electrode (WE, nickel). The circuit potentials (*V*) are reported with respect to the reference electrode. The working electrode was a

nickel wire (Goodfellow, 99.98%) embedded in epoxy. The electrode array was wet polished before experiments, and the reactions took place at the end of the electrode. The diameter of the nickel working electrode was 1 mm. The experiments were performed at room temperature.

For bipolar electrodes, a closed setup was used as shown in Fig. 1b, with a Hg/Hg_2SO_4 sat. K_2SO_4 reference, and two platinum coated titanium rods as driving electrodes. The two compartments in the cell were separated by a bipolar electrode (nickel) embedded in insulator (epoxy). The driving electrode on the right side was connected to the working point of a potentiostat; this side became the cathode of the bipolar electrode. The driving electrode on the left side was connected to the counter point of a potentiostat; this side became the anode of the bipolar electrode. A picture of the experimental setup is shown in Fig. 1c, and an optical image of the nickel BPE embedded in epoxy is shown in Fig. 1d.

The frequency of the oscillations was calculated based on phase description of oscillators; 28 the Hilbert transform of the time series of a signal x

$$H(t) = \frac{1}{\pi} PV \int_{-\infty}^{\infty} \frac{x(\tau) - \langle x \rangle}{t - \tau} d\tau$$
 [1]

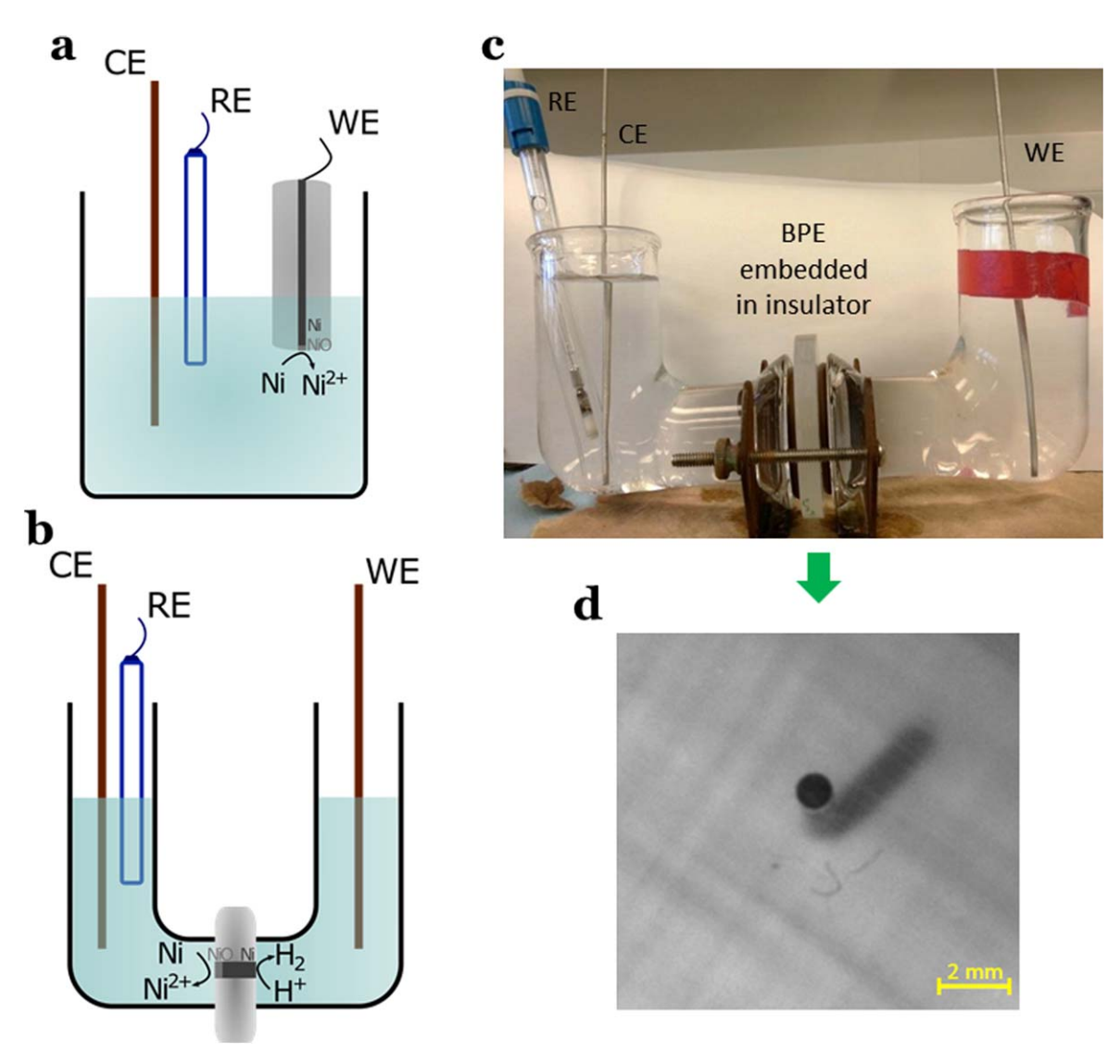


Figure 1. Schematic diagram of experimental setup in traditional cell and in BPE. (a) Experimental setup in traditional cell. WE: Working electrode (nickel); RE: Reference electrode (Hg/Hg_2SO_4 sat. K_2SO_4); CE: Counter electrode (Hg/Hg_2SO_4 sat. Hg/Hg_2SO_4 sat. Hg

was used in defining the phase²⁸

$$\phi(t) = \arctan \frac{H(x(t))}{x(t) - \langle x \rangle}$$
 [2]

where PV in the equation implies that the integral should be evaluated in the sense of Cauchy principal value. $\langle x \rangle$ is the temporal average of the time series x(t). x is the current (x(t) = I(t)). The natural frequency of the oscillator was obtained from a linear fit of $\phi(t)$ vs. t

$$\omega = \frac{1}{2\pi} \left\langle \frac{d\phi}{dt} \right\rangle \tag{3}$$

Results and Discussion

The results are first presented for nickel electrodissolution in a traditional three electrode cell (i.e., anodic reaction not coupled to hydrogen ion reduction), so that the dynamics of the coupled system in BPE can be better understood.

Nickel electrodissolution in traditional cell.—In a traditional cell, a 1 mm diameter nickel wire, immersed in the electrolyte was used as a working electrode in a three-electrode configuration. (See Fig. 1 and the Methods Section for further details).

Oscillations with 3M H_2SO_4 .—Figure 2a shows a linear sweep voltammogram (LSV) with c = 3M H_2SO_4 electrolyte in the transpassive metal dissolution region. With increasing the circuit potential

(V), the current increases due to the increased metal dissolution rate through the oxide film. At V=1.15 V a current peak is recorded, after which the current decreases with increasing potential until V=1.20 V. This is the so-called negative differential resistance region; above this region the current increases again due to water electrolysis. Note that the NDR region starts at an overpotential of about $\eta_a \approx 1.8$ V considering the open circuit potential (OCP) of the electrode ($V_{\rm OCP}=-0.64$ V vs Hg/Hg₂SO₄/sat. K₂SO₄).

In the nickel electrodissolution system, oscillation can occur in a potential region just below the NDR region (where the negative slope is hidden by other reactions, i.e., $\eta_a \approx 1.7~\rm V$) when sufficiently large ohmic IR drop is present in the cell. ^{29,30} Such IR drop can be induced by attaching an external resistance to working electrode. Figure 2b shows the LSV with an external resistance $R_{\rm ext} = 150~\Omega$ attached to the working electrode. Current oscillation can be observed in a 165 mV range of circuit potential (1.084 V < V < 1.249 V) with a current level of I=0.553 mA at the beginning and 0.814 mA at the end of the region, respectively. Note that the oscillation start and end with zero amplitude and finite frequency, which is a characteristic of a supercritial Hopf bifurcation. ²⁹

When a somewhat larger external resistance ($R_{ext} = 262 \Omega$, see Fig. 2c) was attached to the working electrode, a larger oscillatory circuit potential region (202 mV) was observed. In addition, note that while the onset of oscillation is through a Hopf bifurcation (i.e., with small amplitude and finite frequency), the oscillations cease abruptly with a finite amplitude and large period—this transition is consistent with a homoclinic (saddle-loop) bifurcation. ²⁹ Close to the homoclinic bifurcation the shape of the current oscillations are more deformed and develop a relaxation character with slowing down at low, and speeding up at large current levels.

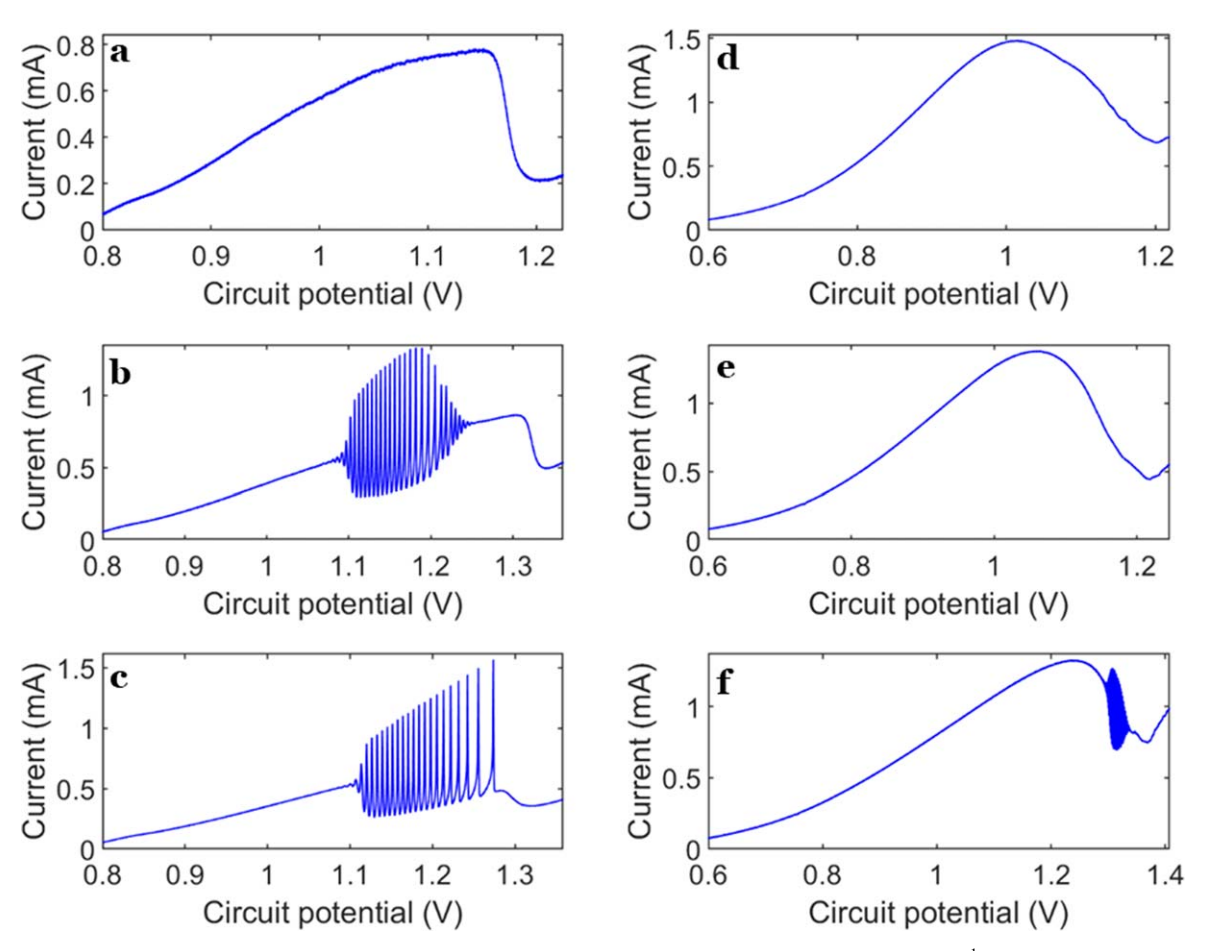


Figure 2. Nickel electrodissolution in traditional cell. (a)–(c) 3 M H₂SO₄; (d)–(f) 6 M H₂SO₄. Scan rate: 10 mV s⁻¹. (a) $R_{\rm ext} = 0$ Ω. (b) $R_{\rm ext} = 150$ Ω. (c) $R_{\rm ext} = 262$ Ω. (d) $R_{\rm ext} = 0$ Ω. (e) $R_{\rm ext} = 37$ Ω. (f) $R_{\rm ext} = 170$ Ω.

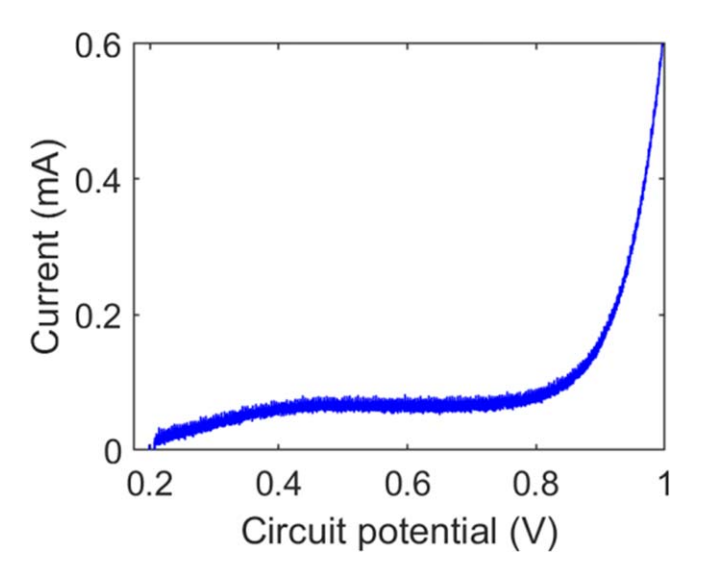


Figure 3. Linear sweep voltammogram of the driving electrode (Pt) in the U-cell with $3M\ H_2SO_4$. Scan rate: $1\ mV\ s^{-1}$.

Oscillations with 6M H₂SO₄.—Similar experiments were performed with c=6 M H_2SO_4 shown in Figs. 2d-2f. The nickel electrodissolution is acid catalyzed, 31 and thus larger currents can be expected at this higher concentration. Figure 2d shows a LSV without external resistance in the transpassive dissolution region. The current increased with increasing the circuit potential until a peak current of I = 1.478mA was observed at V = 1.024 V, with no oscillatory behavior. Compared to the scan shown in Fig. 2a with 3M H₂SO₄, the current level is increased by 89.5% when the concentration of acid is doubled. Note also that the NDR region is wider giving a smaller slope (in magnitude) than at the lower acid concentration. Figure 2e shows the LSV when a small amount of external resistance $(R_{ext} = 37 \Omega)$ is added to the system. There are no oscillations and the current level is slightly lower compared to Fig. 2d with a peak current of 1.385 mA. When an external resistance ($R_{ext} = 170 \Omega$) is added as shown in Fig. 2f, current oscillations occur, but on the negative slope in a small circuit potential range of about 50 mV, with a current level of I = 1.198 mA to 0.824 mA. The oscillation start and end with Hopf bifurcations under these conditions.

We thus see that with $c=3\mathrm{M}$ H₂SO₄ electrolyte the nickel electrodissolution (in the given cell) does not produce oscillations without added external resistance, with relatively small $R_{\mathrm{ext}}=150~\Omega$ external resistance the oscillation arise and cease through Hopf bifurcations, and at large external resistance $R_{ext}=262~\Omega$ the oscillatory region is larger, and the oscillations cease through a homoclinic bifurcation instead of Hopf. At the increased sulfuric acid concentration of $c=6\mathrm{M}$ H₂SO₄ the oscillation start to arise with about $R_{ext}=170~\Omega$ and typically arise on the negative slope of the polarization scan.

Nickel electrodissolution with BPE.—A BPE electrode was constructed, in which a 1 mm diameter Ni was embedded in epoxy, and the two ends of the wire accommodated the anodic and the cathodic reactions as shown in Figs. 1b–1d. (See the Methods Section for further details.) The counter and reference electrodes were placed in the chamber of a U-cell with the anodic end of the BPE; because here we have a reference electrode, the impact of the counter electrode, which evolves hydrogen, is minimized. The chamber with the cathodic end of the BPE accommodated the working driving electrode, which is polarized anodically (V > 0) and thus oxygen evolution reaction takes place. (Note that in order to realize the BPE, the counter/reference electrodes should be placed in the same compartment, opposite of the WE, so that the circuit potential between the WE and RE includes the potential drop occurs across the BPE.) The current-potential response of the this driving Pt electrode in the

U-cell (without BPE separating the two compartments) was determined to evaluate its effect on the cell dynamics. As shown in Fig. 3, the open circuit potential is around $V_{\rm OCP}=0.20\,$ V. It takes about $V=1\,$ V circuit potential to drive I0.55 mA current. Therefore, it takes about $\eta_D=0.8\,$ V overpotential for the driving electrode to provide the sufficient amount of current for nickel electrodissolution to take place in the transpassive region. This overpotential will have to be considered in decrypting the oscillatory regions in the BPE setting.

Current oscillations with BPE.—First we consider the nickel BPE in the U-cell with 3M $\rm H_2SO_4$ on both sides. The open circuit potential was 0.200 V. The LSV in the transpassive dissolution range is shown in Fig. 4a. Current oscillations were observed in a 160 mV range for 3.10 V < V < 3.26 V. (Considering the OCP, the oscillation start at an overpotential of about 2.9 V.) The current level at the onset of oscillation is 0.550 mA. Figure 4b shows a time series of the oscillatory behavior close to the onset (V = 3.130V). The oscillation waveforms are smooth (nearly harmonic) with a frequency of 1.093 Hz. The mean current is 0.533 mA with an amplitude of 0.201 mA.

We thus see that the BPE behaves fundamentally different from a traditional electrochemical cell. Here, oscillation can occur even without added external resistance. As a working hypothesis, we assume that these oscillations are induced by the hidden NDR, and the minimum required resistance for the oscillations can be provided by the charge transfer resistance of the cathode side of the BPE and the solution resistance. Moreover, the circuit potential at which the oscillations occur is very large, about 3 V, and should consist of the overpotentials needed to drive oscillatory transpassive nickel electrodissolution (η_a), hydrogen ion reduction on the cathode side (η_c), that of the driving electrode to provide sufficient current (η_D), and the ohmic IR drop in the electrolyte:

$$V = \eta_a - \eta_c + \eta_D + IR_s \tag{4}$$

Note that the solution IR contribution is relatively small (on the order of mV), because of the large concentration of the acid and the small solution resistance on the order of $R_s \approx 30 \ \Omega$.

To explore the origin of the spontaneous oscillation in the BPE cell, we performed a cathodic scan in a traditional three electrode cell to determine the charge transfer resistance of the cathodic reaction, hydrogen ion reduction. The LSV is shown in Fig. 4c. As expected the current increases in an exponential manner at large negative overpotentials. In the oscillatory range, the anodic current is about 0.55 mA, and thus the cathodic side of the BPE provides I=-0.55 mA, and this current level occurs at a cathodic overpotential of $\eta_c=-0.4$ V. Now the overpotential for the observed oscillation can be calculated with $\eta_a=1.7$ V, $\eta_c=-0.4$ V, and $\eta_D=0.8$ V using Equation 4; V=2.9 V which agrees will with the experimentally observed value (2.9 V).

Our next step is to evaluate the total cell resistance (R_{tot}) in the BPE setup to confirm that R_{tot} is large enough to allow for the oscillations to occur. R_{tot} is the sum of the charge transfer (R_{ct}) and the solution (R_{s})resistance:

$$R_{\text{tot}} = R_{\text{ct}} + R_{\text{s}} \tag{5}$$

The LSV of the cathode is shown in Fig. 4c; at the current level of the oscillations (I=-0.550 mA), $R_{\rm tot}=153~\Omega$ was obtained from the inverse slope of the polarization curve. Electrochemical impedance spectroscopy (EIS) was further performed to verify the resistance and separate $R_{\rm tot}$ into the solution and charge transfer resistances. As shown in Fig. 4d, an EIS was performed at $V=-1.05~\rm V$, which corresponds to $I=-0.550~\rm mA$. From the Randles equivalent circuit (semicircle in the Nyquist plot) fit, $^3R_s=31~\Omega$, $R_{tot}=R_{ct}+R_s=150~\Omega$, and thus $R_{ct}=119~\Omega$. The total resistance (153 Ω) measured by the slope of the cathodic scan is in accordance with the resistance (150 Ω) found by EIS. These observation indicate that the charge transfer resistance of the cathodic reaction, $R_{ct}=119~\Omega$, contributes largely to the $R_{tot}=150~\Omega$.

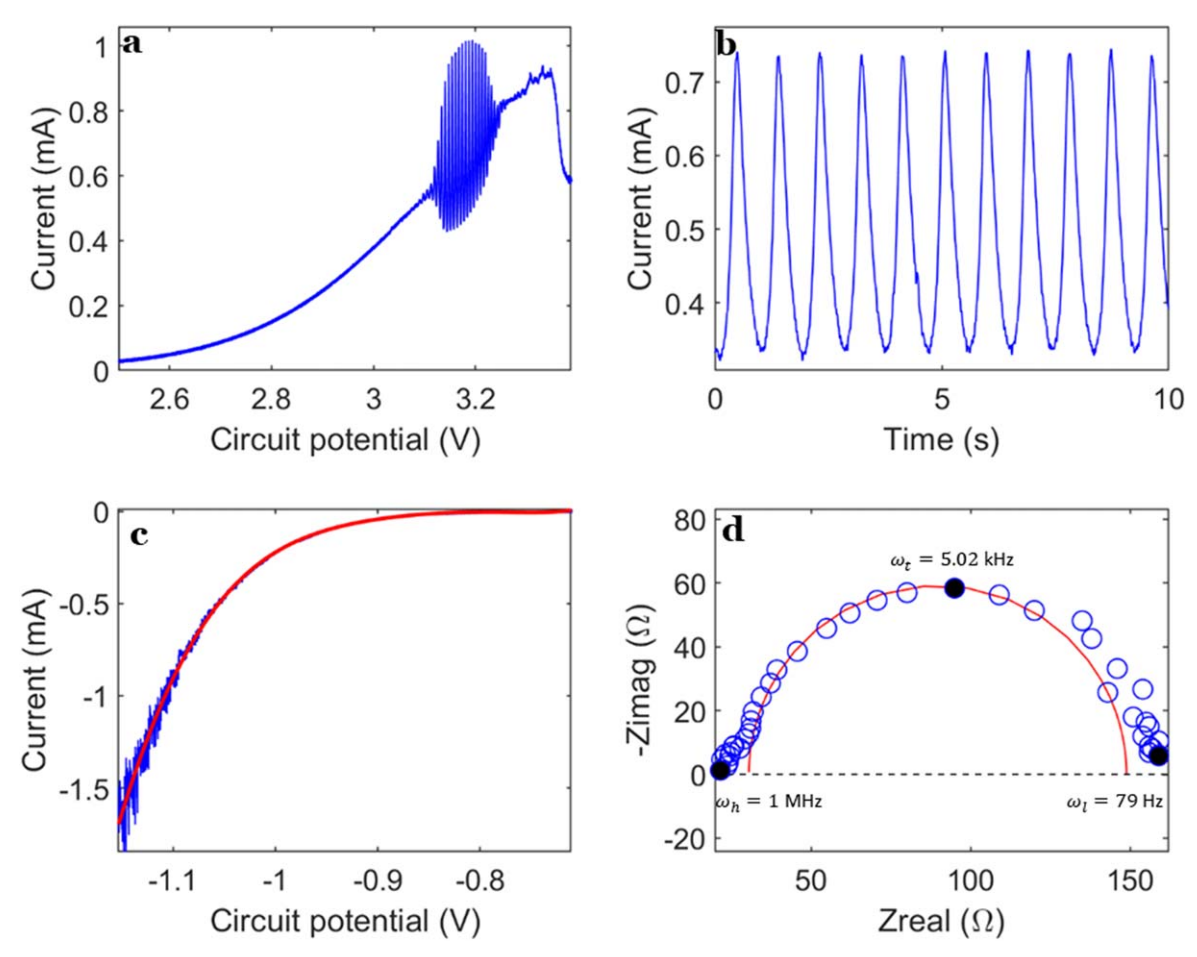


Figure 4. Nickel electrodissolution in BPE (3M H_2SO_4 |Ni|3M H_2SO_4). (a) Linear sweep voltammogram. Scan rate: 10 mV s⁻¹. (b) Current oscillation vs time at V = 3.13 V. (c) Cathodic scan of nickel electrode in traditional cell. Scan rate: 1 mV s⁻¹. (d) Nyquist plot of EIS obtained at V = -1.05 V in the traditional cell.

As the experiments with the traditional setup Fig. 2b showed, the nickel dissolution system exhibits oscillations starting and ending with Hopf bifurcation in a circuit potential range of 165 mV in the presence of $R_{ext} = 150 \Omega$ resistance. This agrees well with the BPE results with the oscillations through Hopf bifurcation, with a range of 165 mV. We also showed that the oscillations occur at overpotentials that drive the anodic side of the BPE to the NDR region. The results with the BPE are thus consistent with oscillations emanating from the NDR of the anodic dissolution reaction, with the cathodic end (and the cell solution resistance to a lesser extent) providing the necessary total cells resistance for the oscillations. We should emphasize that in addition to the remarkable similarities between Figs. 2b and 4a, there are also differences, which are not captured by the simple model. While the total resistance with the traditional setup is nearly constant with increasing the potential, in the BPE the R_{ct} depends on the current level. Previously, it was shown²⁵ that the effective R_{ct} for a Butler-Volmer kinetics at large overpotentials is inversely proportional to the current level:

$$R_{\rm ct} = \frac{RT}{\alpha F |I_c|}$$
 [6]

where R is gas constant, T is temperature, α is the transfer coefficient, and I_c is the cathodic current level. Therefore, at small current the coupled cathode-anode system experiences large resistance, which is diminished with increasing the current. This can be seen in Fig. 4a: the current increases with increasing V with a positive curvature (and thus indicating progressively less resistance), instead of the nearly linear increase with constant resistance in

Fig. 2b). Therefore, while many of the features of the BPE system can be captured by overpotential and $R_{\rm ct}$ predictions, we anticipate that, generally speaking, not all dynamical states could be equivalent in the traditional setup and the BPE.

The BPE setup allows varying the anodic and cathodic side electrolyte compositions relatively easily, which facilitates the investigation of nonlinear phenomena in a large parameter space. Here we demonstrate two such examples, one with decreasing the acid concentration (c) on the cathode side, and the other with increasing c on the anode side. These two conditions were chosen as they typically both increase the IR drop in a traditional cell, the former by increasing the solution resistance, and the latter by increasing the current. As with increasing the IR drop the nickel electrodissolutin is expected to oscillate in larger circuit potential regions, 29 the initial expectations were that both would promote instabilities in the BPE cell as well.

Effect of decreasing sulfuric acid concentration on cathode side.— The LSV in the transpassive dissolution region is shown in Fig. 5a with 3M $\rm H_2SO_4$ on the anodic, and 0.1M $\rm H_2SO_4$ on the cathodic side. Current oscillation is again observed for 3.250 V < V < 3.502 V. The oscillation start with Hopf bifurcation and end with homoclinic bifurcation with a circuit potential range of 252 mV. The current level at the onset of oscillation is 0.545 mA. The current oscillation waveform has a strong relaxational character as shown in Fig. 5b with a frequency of 0.768 Hz. The mean current is 1.102 mA with an amplitude of 0.500 mA. Both the mean current and the amplitude are larger than those in Fig. 4b, where the oscillations are smooth and occur at lower V.

Another cathodic scan in a traditional cell was performed to determine the resistance of the cathodic side in the decreased acid

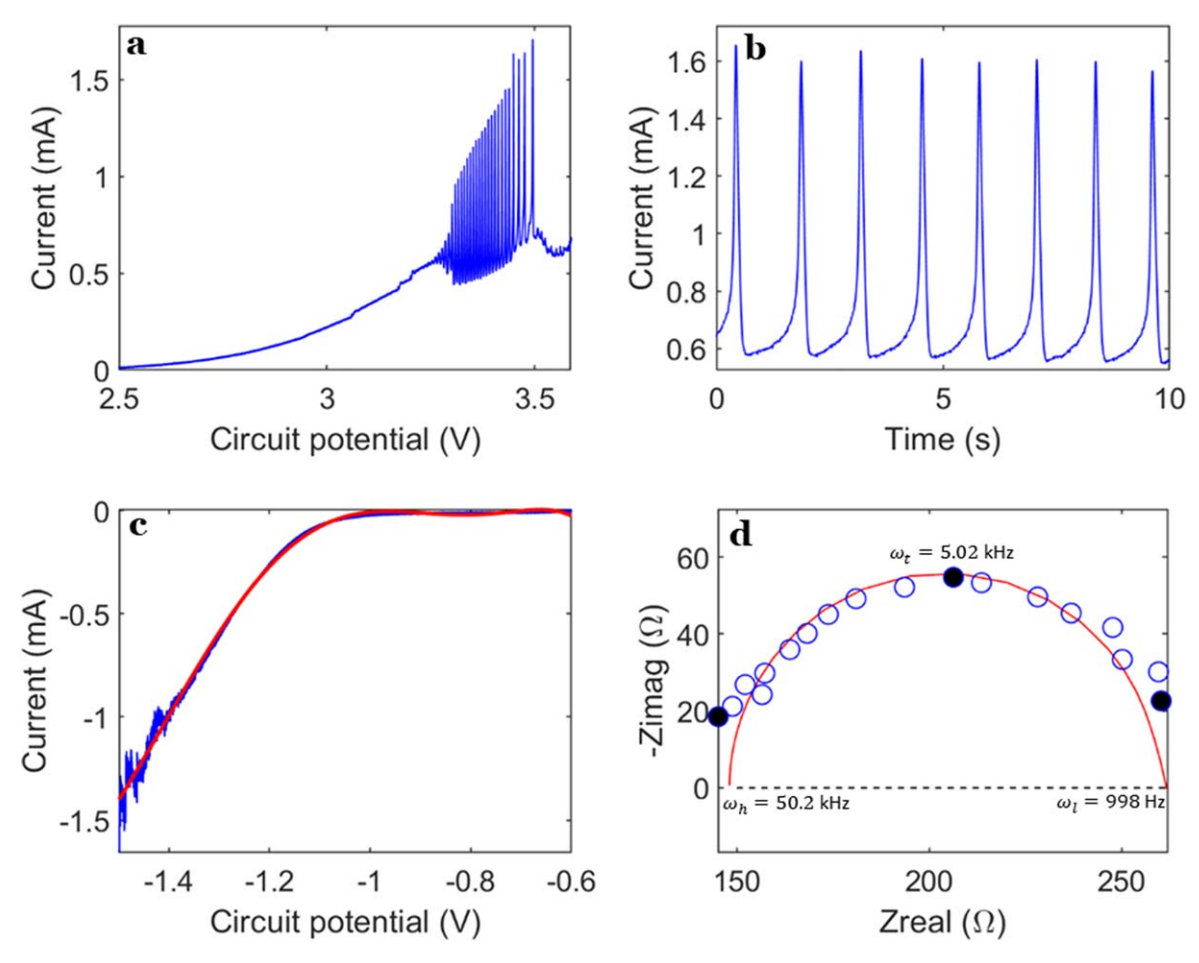


Figure 5. Nickel electrodissolution in BPE with decreased acid concentration at the cathodic side (3M $H_2SO_4|Ni|0.1M$ H_2SO_4). (a) Linear sweep voltammogram. (b) Current oscillation vs time at V = 3.23 V. (c) Cathodic scan of nickel electrode in traditional cell. Scan rate: 1 mV s⁻¹. (d) Nyquist plot of EIS obtained at V = -1.29 V.

concentration (c = 0.1 M)as shown in Fig. 5c. The inverse of the slope (275 Ω) was determined at the current level (0.545 mA) where the onset of current oscillation was observed in Fig. 5a. As shown in Fig. 5d, EIS was performed at V = -1.29 V, corresponding to the cathodic current I = -0.545 mA expected from the oscillations in Fig. 5a. It was found that for $c = 0.1 \text{ M} \text{ H}_2\text{SO}_4$, the solution resistance is $R_s = 148 \Omega$, and the total resistance is $R_{tot} = R_s + R_{ct} = 262 \Omega$, and thus $R_{ct} = 114 \Omega$. The total resistance (275 Ω) measured by the slope of the cathodic scan is close to the resistance (262 Ω) found by EIS. We note that in this case, about half of the total external resistance is provided by the solution resistance. The current oscillations obtained in the BPE setup thus can be compared to the oscillations in the traditional setup with $R_{\rm ext} = 262~\Omega$, shown in Fig. 2c. Both polarization scans show Hopf and homoclinic bifurcations at the beginning and at the end of the oscillations, respectively, with similar ranges (202 mV vs 252 mV in BPE), and emergence of relaxation oscillations. Note that the BPE oscillation range is somewhat larger, which can be contributed to the nonlinear dependence of the charge transfer resistance on the current level discussed above. Overall, there is excellent agreement between the predicted behavior from the traditional setup and the observed behavior with BPE.

Lowering the acid concentration thus generates polarization scans that mimics oscillations in the traditional setup observed at a larger total resistance. This could be expected because decreasing the acid concentration increases the solution and charge transfer resistance of the hydrogen ion reduction reaction. Note that because of the BPE configuration and the large cathodic overpotential, the experimentally measured R_{ct} value remained nearly the same (in fact, decreased slightly from 119 Ω to 114 Ω); this nearly constant

value is in agreement with the prediction of Equation 6. Thus, in this case, the change of the features of the oscillations (due to change of R_{tot}) are nearly fully contributed to the change in the solution resistance. As such, we would expect that further decrease in the acid concentration would further increase the cell series resistance, and the oscillation would occur at progressively larger potentials until mass transport limitations start to play a role.

Effect of increasing the sulfuric acid concentration on the anode side.—When the concentration of the sulfuric acid on the anode side is changed, the current level required for the oscillations can also change, which should be incorporated in the analysis. Figure 6 shows the BPE results with 6 M H₂SO₄ on the anodic, and 3M H₂SO₄ on the cathodic side. The LSV in the transpassive dissolution region is shown in Fig. 6a. In this case, oscillations do not occur. As expected, higher current levels are measured than those observed with the 3M H₂SO₄. EIS results obtained at V = -1 V, where the same current level is obtained in a cathodic scan as the peak current in Fig. 6a, are shown in Fig. 6b. The solution resistance was R_s = 11 Ω , the total resistance was $R_{tot} = R_s + R_{ct} = 37 \Omega$, and thus $R_{ct} = 26 \Omega$. This small external resistance cannot induce oscillations in Ni dissolution in traditional setup (see Fig. 2e). The lack of oscillations in the BPE setup at increased current oscillations thus can be contributed to the decreased charge transfer resistance of the cathode at the high current level, as predicted by Equation 6. While the traditional setup generates oscillations at both c = 3 and 6 M with similar external resistances, in the BPE setup the higher current level and thus lower charge transfer resistance of the cathode does not provide the sufficient feedback for spontaneous oscillations to occur.

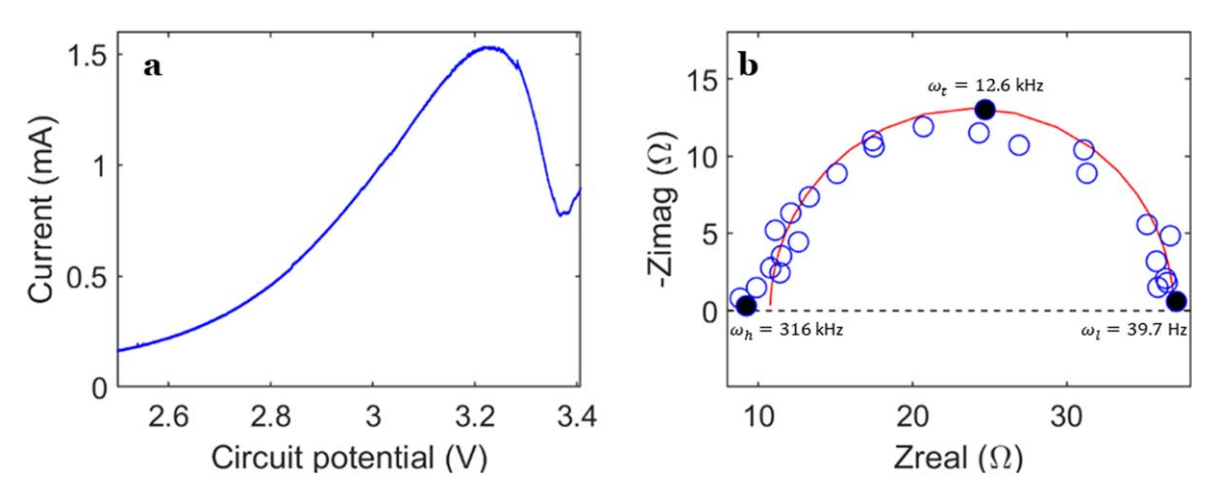


Figure 6. Nickel electrodissolution in BPE with increased acid concentration at the anodic side (6 M $H_2SO_4|Ni|3M$ H_2SO_4). (a) Linear sweep voltammogram. Scan rate: 1 mV s⁻¹. (b) Nyquist plot of EIS obtained at V = -1.00 V.

Conclusions

The nonlinear dynamics of a coupled cathode-anode reaction in a bipolar electrode setting was decoded. Compared to the traditional setting where external resistance was required to induce oscillations. in BPE the cathode reaction can facilitate the emergence of oscillatory instabilities even without an external resistance. In the BPE, a larger circuit potential is required to drive the reactions, as a result of the additional overpotentials required for the cathodic reaction and the driving electrodes. By tuning the concentration in the cathodic and the anodic chambers, the dynamics and oscillatory range can be changed. The analysis of the charge transfer resistance of the fast process (in our case, the hydrogen ion reduction reaction) along with measurements of solution resistance (e.g., with EIS) can interpret and predict the occurrence of oscillations. In this respect, the results are similar to those observed with the coupling of the cathode and the anode in a proton-exchange fuel cell.³² where one reaction, in that case, the anodic reactions, drove the oscillations, and the cathodic process reacted, i.e., "synchronized". Resolving cathode and anode potentials in both BPE and fuel cells can provide valuable information about the coupling of the electrodes.

In addition to oscillations, the BPE could also be used to study bistability when considering forward and backward scans in the LSV; here new factors should be considered, in particular, the current level affects the charge transfer resistance of the coupled electrode and thus the interpretation of the bistability ranges induced by saddle-node bifurcations should consider that the imposed charge transfer resistance depends on the current level.²⁵

The wireless feature of the BPE can open novel routes to studying nonlinear dynamics in electrochemistry; this feature is similar to coupling chemical reactions to obtain new types of behavior, as it was demonstrated with coupling of two reactors with the chlorite-iodide reaction for rhythmogenesis, ³³ and the parallel coupled bromate-chlorite-idode system for birythmicity and compound oscillations. ³⁴ Here we used a reference state where both compartments contained 3M H₂SO₄ and changed the concentration in one of the compartments; future studies could explore the impact of antagonistic changes in both compartments, e.g., increasing the concentration in one compartment at the expense of decreasing the concentration in the other.

The BPE also allows investigations of electrode arrays without complicated multichannel potentiostats, for example, through optical recordings using fluorescence.²⁰

Acknowledgments

IZK acknowledges support from the National Science Foundation (NSF) (Grant No. CHE-1900011).

ORCID

István Z. Kiss https://orcid.org/0000-0003-0993-3184

References

- 1. J. Hudson and T. Tsotsis, Chem. Eng. Sci., 49, 1493 (1994).
- K. Krischer, Modern Aspects of Electrochemistry, ed. B. E. Conway et al. (Springer, US) Vol. 32, p. 1 (2002).
- A. J. Bard and L. R. Faulkner, Electrochemical Methods: Fundamentals and Applications (Wiley) 2nd ed. (2001).
- M. Orlik, Self-Organization in Electrochemical Systems I (Springer-Verlag, Berlin, Heidelberg) (2012).
- M. Orlik, Self-Organization in Electrochemical Systems II (Springer-Verlag, Berlin, Heidelberg) (2012).
- K. Krischer and H. Varela, Handbook of Fuel Cells, ed. W. Vielstich et al. (American Cancer Society) (2010).
- 7. I. Z. Kiss, Y. Zhai, and J. L. Hudson, *Science*, **296**, 1676 (2002).
- 8. J. M. Cruz, M. Rivera, and P. Parmananda, *Phys. Rev. E*, **75**, 035201 (2007).
- S. Bozdech, Y. Biecher, E. R. Savinova, R. Schuster, K. Krischer, and A. Bonnefont, *Chaos*, 28, 045113 (2018).
- 10. A. G. Cioffi, R. S. Martin, and I. Z. Kiss, J. Electroanal. Chem., 659, 92 (2011).
- 11. P. Sun and M. V. Mirkin, *Anal. Chem.*, **78**, 6526 (2006).
- W. Wang, J. Zhang, F. Wang, B. W. Mao, D. Zhan, and Z. Q. Tian, J. Am. Chem. Soc., 138, 9057 (2016).
- M. A. Edwards, D. A. Robinson, H. Ren, C. G. Cheyne, C. S. Tan, and H. S. White, Faraday Discuss., 210, 9 (2018).
- Faraday Discuss., 210, 9 (2018).

 14. J. R. Backhurst, J. M. Coulson, F. Goodridge, R. E. Plimley, and M. Fleischmann,
- J. Electrochem. Soc., 116, 1600 (1969).
 M. Fleischmann, J. Ghoroghchian, D. Rolison, and S. Pons, J. Phys. Chem., 90, 6392 (1986).
- S. E. Fosdick, K. N. Knust, K. Scida, and R. M. Crooks, *Angew. Chem. Int. Ed.*, 52, 10438 (2013).
- 17. L. Koefoed, S. U. Pedersen, and K. Daasbierg, *Curr. Opinion Electrochem.*, **2**, 13 (2017).
- 18. A. Arora, J. C. T. Eijkel, W. E. Morf, and A. Manz, *Anal. Chem.*, **73**, 3282 (2001).
- 19. R. Hao, Y. Fan, C. Han, and B. Zhang, Anal. Chem., 89, 12652 (2017).
- 20. J. P. Guerrette, S. J. Percival, and B. Zhang, J. Am. Chem. Soc., 135, 855 (2013).
- 21. J. T. Cox, J. P. Guerrette, and B. Zhang, *Anal. Chem.*, **84**, 8797 (2012).
- 22. B. A. Frontana-Uribe, R. D. Little, J. G. Ibanez, A. Palma, and R. Vasquez-Medrano, *Green Chem.*, **12**, 2099 (2010).
- M. J. Llorente, B. H. Nguyen, C. P. Kubiak, and K. D. Moeller, *J. Am. Chem. Soc.*, 138, 15110 (2016).
- T. Wu, B. H. Nguyen, M. C. Daugherty, and K. D. Moeller, *Angew. Chem. Int. Ed.*, 58, 3562 (2019).
- 25. M. Wickramasinghe and I. Z. Kiss, J. Electrochem. Soc., 163, H1171 (2016).
- M. J. Hankins, M. Wickramasinghe, and I. Z. Kiss, *Electrochim. Acta*, 252, 76 (2017).
- 27. M. J. Hankins, V. Gáspár, and I. Z. Kiss, *Chaos*, 29, 033114 (2019).
- A. Pikovsky, M. Rosenblum, and J. Kurths, Synchronization: A Universal Concept in Nonlinear Sciences (Cambrige University Press, Cambrige, UK) (2001).
- 29. I. Z. Kiss, Z. Kazsu, and V. Gáspár, *Chaos*, 16, 033109 (2006).
- 30. M. T. M. Koper, Adv. Chem. Phys., 92, 161 (1996).
- D. Haim, O. Lev, L. M. Pismen, and M. Sheintuch, J. Phys. Chem., 96, 2676 (1992).
- 32. J. A. Nogueira, K. Krischer, and H. Varela, ChemPhysChem, 20, 3081 (2019).
- M. Boukalouch, J. Elezgaray, A. Arneodo, J. Boissonade, and P. De Kepper, J. Phys. Chem., 91, 5843 (1987).
- 34. M. Alamgir and I. R. Epstein, J. Am. Chem. Soc., 105, 2500 (1983).